

Effect of composition on magnetocaloric properties of $\text{Mn}_3\text{Ga}(1-x)\text{Sn}_x\text{C}$

E. T. Dias, K. R. Priolkar, Ö. Çakir, M. Acet, and A. K. Nigam

Citation: *Journal of Applied Physics* **117**, 123901 (2015); doi: 10.1063/1.4916095

View online: <http://dx.doi.org/10.1063/1.4916095>

View Table of Contents: <http://scitation.aip.org/content/aip/journal/jap/117/12?ver=pdfcov>

Published by the [AIP Publishing](#)

Articles you may be interested in

[Negative and conventional magnetocaloric effects of a MnRhAs single crystal](#)

J. Appl. Phys. **115**, 203909 (2014); 10.1063/1.4880397

[Reversibility in the inverse magnetocaloric effect in Mn₃GaC studied by direct adiabatic temperature-change measurements](#)

Appl. Phys. Lett. **100**, 202404 (2012); 10.1063/1.4717181

[Magnetostructural phase transitions and magnetocaloric effects in MnNiGe_{1-x}Al_x](#)

Appl. Phys. Lett. **100**, 052404 (2012); 10.1063/1.3681798

[Effect of impurity doping at the Mn-site on magnetocaloric effect in Pr_{0.6}Ca_{0.4}Mn_{0.96}B_{0.04}O₃ \(B = Al, Fe, Cr, Ni, Co, and Ru\)](#)

J. Appl. Phys. **109**, 023903 (2011); 10.1063/1.3531987

[Negative magnetocaloric effect at the antiferromagnetic to ferromagnetic transition of Mn₃GaC](#)

J. Appl. Phys. **94**, 1800 (2003); 10.1063/1.1587265

A promotional banner for the Journal of Applied Physics. It features the AIP logo and the text 'Journal of Applied Physics' at the top. Below this, it says 'Meet The New Deputy Editors'. Three circular portraits of the new deputy editors are shown: Christian Brosseau, Laurie McNeil, and Simon Phillpot. The background is a dark orange with a pattern of colorful, abstract shapes.

Effect of composition on magnetocaloric properties of $\text{Mn}_3\text{Ga}_{(1-x)}\text{Sn}_x\text{C}$

E. T. Dias,¹ K. R. Priolkar,^{1,a)} Ö. Çakir,² M. Acet,³ and A. K. Nigam⁴

¹Department of Physics, Goa University, Goa 403206, India

²Physics Department, Yildiz Technical University, TR-34220 Esenler, Istanbul, Turkey

³Faculty of Physics and CENIDE, Universitat Duisburg-Essen, D-47048 Duisburg, Germany

⁴Tata Institute of Fundamental Research, Dr. Homi Bhabha Road, Colaba, Mumbai 400005, India

(Received 22 February 2015; accepted 12 March 2015; published online 23 March 2015)

A study investigating the effect of Sn substitution on the magnetocaloric properties of $\text{Mn}_3\text{Ga}_{(1-x)}\text{Sn}_x\text{C}$ compounds reveals that the nature of the magnetocaloric effect (MCE) has a strong dependence on the nature of the magnetic ordering. For small amounts of Sn ($x \leq 0.2$), the MCE is of the inverse type, wherein an increase in the applied field beyond 5 T gives rise to a table like temperature dependence of the entropy due to a coupling between the first order ferromagnetic (FM)–antiferromagnetic (AFM) transition and the field induced AFM–FM transition. Replacement of Ga by larger concentrations of Sn ($x \geq 0.71$) results in a change of the MCE to a conventional type with very little variation in the position of $(\Delta S_M)_{max}$ with increasing magnetic field. This has been explained to be due to the introduction of local strain by A site ions (Ga/Sn), which affect the magnetostructural coupling in these compounds. © 2015 AIP Publishing LLC.

[<http://dx.doi.org/10.1063/1.4916095>]

I. INTRODUCTION

The magnetocaloric effect (MCE) that is intrinsic to all magnetic materials is due to the coupling of magnetic sublattice with the magnetic field¹ and can be characterized directly by measuring adiabatic change in temperature (ΔT_{ad}) upon application of magnetic field,^{2,3} or indirectly from heat capacity measurements, or by estimating the isothermal entropy changes (ΔS_M) due to changes in applied magnetic field. Although this effect has been historically used in production of low temperatures, the discovery of giant magnetocaloric effect in $\text{Gd}_5\text{Si}_2\text{Ge}_2$ ⁴ has stimulated both basic and applied interest in the development of new materials that are useful for room temperature magnetic refrigeration as an alternative to vapor-compression technology.⁵

For the purpose of practical application, a magnetocaloric material must have comparatively large MCE values in small fields ($H \leq 2\text{ T}$), accompanying a first order transition preferably near room temperature along with a minimum thermal hysteresis to ensure the life span of the magnetic refrigerator upon cyclically applying and removing external magnetic fields.⁶ Apart from $\text{Gd}_5(\text{Si}_x\text{Ge}_{(1-x)})_4$, other known systems with considerable MCE values around room temperature include lanthanum manganese perovskite oxides,⁷ transition metal based alloys,^{8,9} Heusler alloys,^{10–12} and 3d transition metal rich systems with values comparable to those of Gd.^{13,14} These results include $\text{MnFeP}_{(1-x)}\text{As}_x$ system exhibiting reversible giant magnetic entropy change with the same magnitude as $\text{Gd}_5\text{Si}_2\text{Ge}_2$ ¹⁵ and renewed interest in materials exhibiting considerable magnetic entropy change at temperatures corresponding to their first order magnetic transitions.^{15,16}

Another class of materials that have attracted attention as candidates for ferroic cooling applications are the Mn

based antiperovskite materials. Amongst these Mn_3GaC , undergoes a volume discontinuous first order transition from a ferromagnetic (FM) to an antiferromagnetic (AFM) ground state at 160 K,^{17,18} accompanied by a large MCE in relatively low fields¹⁹ as well as a table like MCE in high fields preferred when designing a practical refrigerant unit.²⁰

On the other hand, Mn_3SnC exhibits a sharp first order change from a paramagnetic (PM) state to a noncollinear ferrimagnetic (FIM) state at $\sim 279\text{ K}$, accompanied by a conventional magnetic entropy change ($80.69\text{ mJ/cm}^3\text{ K}$ and $133\text{ mJ/cm}^3\text{ K}$ under a magnetic field of 2 T and of 4.8 T).^{18,21} These materials are not only interesting from a technological point of view but also to understand the nature of magneto-structural coupling present in these antiperovskites. Prior to the first order transformation from a low volume cubic FM phase to high volume cubic AFM phase, Mn_3GaC undergoes a second order PM to FM transition at about 248 K. The relative strengths of these two transitions can be modulated by controlling the carbon stoichiometry²² or even by partial replacement of C by nitrogen.²³ These studies indicate that the magneto-structural coupling is critically dependent on Mn 3d - C 2p band hybridization. Therefore, a drastic change in nature of magnetic order via a replacement of Ga by Sn invokes interest. It has been recently shown that systematic replacement of Ga by Sn results in compounds showing characteristics of both the parent compounds.²⁴ Another interesting aspect of Mn_3GaC is the existence of a completely reversible magnetic field induced first order transition from the high volume AFM state to a low volume FM state.²⁵ Such a transition is absent in Mn_3SnC . As MCE is intimately related to the magneto-structural coupling, here we use it as a tool to understand the nature of magneto-structural coupling in Mn_3GaC and Mn_3SnC . Isothermal magnetic entropy changes under different applied magnetic fields in the vicinity of the first order transitions have been studied in several compositions of

^{a)}Author to whom correspondence should be addressed. Electronic mail: kpr@unigoa.ac.in

$\text{Mn}_3\text{Ga}_{(1-x)}\text{Sn}_x\text{C}$ ($0 \leq x \leq 1$). The results suggest that the magnetostructural coupling in these antiperovskite compounds critically depends on the local strain introduced by the A site cation.

II. EXPERIMENTAL

Isothermal magnetic entropy change associated with a magnetic transition of a material can be calculated from the field dependence of magnetization.²⁶ For this purpose, Sn doped Mn_3GaC type polycrystalline compounds of general formula $\text{Mn}_3\text{Ga}_{(1-x)}\text{Sn}_x\text{C}$ ($0 \leq x \leq 1$) prepared using the solid state reaction method and characterized for their structural, transport, and magnetic properties as described in Ref. 24 were used. Isothermal magnetic entropy change, ΔS_M , was estimated utilizing Maxwell's equation,

$$\left(\frac{\partial S(T, H)}{\partial H}\right)_T = \left(\frac{\partial M(T, H)}{\partial T}\right)_H, \quad (1)$$

which on integration for an isothermal-isobaric process gives

$$\Delta S_M(T, \Delta H) = \int_{H_1}^{H_2} \left(\frac{\partial M(T, H)}{\partial T}\right)_H dH. \quad (2)$$

Isothermal magnetization curves, $M(H)$, were recorded at several temperatures with an interval of 3 K–5 K around the first order transition region.²⁷

The area between two magnetic isotherms recorded at close temperatures obtained from Eq. (2) corresponds to a change in free energy, which on dividing by the temperature interval gives the value of magnetic entropy change corresponding to an average of the two temperatures.³ Magnetization data for $\text{Mn}_3\text{Ga}_{(1-x)}\text{Sn}_x\text{C}$ ($0 \leq x \leq 1$) compounds were recorded using a SQUID magnetometer at temperature intervals of 3 K–5 K. Each measurement as a

function of field (0–7 T) was carried out in zero field cooled (ZFC) mode, wherein the sample was first heated to temperatures above its T_C in the PM state and then cooled to the measuring temperature in the absence of applied field.

III. RESULTS

A detailed analysis of structural and magnetic properties of $\text{Mn}_3\text{Ga}_{(1-x)}\text{Sn}_x\text{C}$ ($0 \leq x \leq 1$) compounds suggests that Sn doping in Mn_3GaC , though does not alter the primitive cubic crystal structure, leads to increase in unit cell volume along with a gradual increase in the strength of FM interactions to a point where the first order transition in Mn_3GaC is completely altered from FM–AFM type to a PM–FIM type in Mn_3SnC .²⁴ This behaviour can also be seen in Figure 1, wherein temperature dependence of magnetization measured in 0.01 T applied field during ZFC and field cooled (FC) cycles is plotted for several compositions of $\text{Mn}_3\text{Ga}_{(1-x)}\text{Sn}_x\text{C}$. With decreasing temperature, the Ga rich compounds, $x \leq 0.23$, first transform from a room temperature PM state to an intermediate FM state via a second order transition before undergoing a first order transition to the AFM ground state. $M(T)$ results for compounds with intermediate concentrations of Ga and Sn ($0.4 \leq x \leq 0.7$) show a co-existence of two magnetic phases: Ga rich phase, which orders antiferromagnetically and a Sn rich phase with dominant ferromagnetic interactions. The strength of FM interactions continues to further increase across the series, while suppressing the AFM state in the Sn rich ($x \geq 0.8$) compounds.

The change in the type of magnetic interactions present in magnetic ground state of $\text{Mn}_3\text{Ga}_{(1-x)}\text{Sn}_x\text{C}$ compounds is further illustrated by magnetization isotherms $M(H)$ recorded in the vicinity of their respective first order transitions and are presented in Figures 2–4. As can be seen in Fig. 2, $M(H)$ for Mn_3GaC ($x=0$) recorded at 175 K exhibits a typical

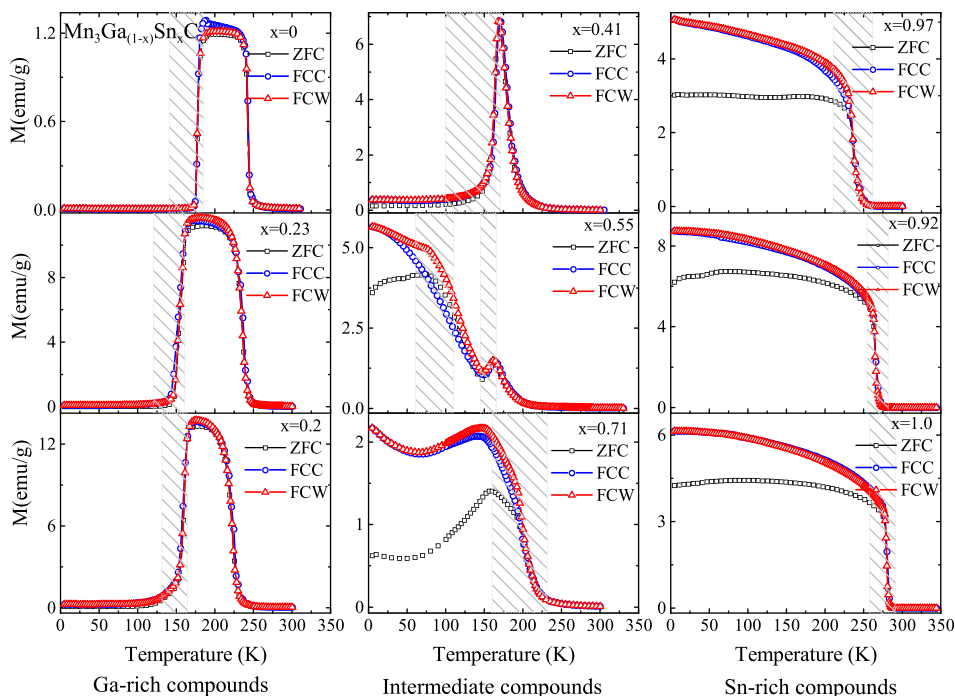


FIG. 1. Temperature dependence of magnetization measured in 0.01 T applied field during ZFC, FCC, and FCW cycles for $\text{Mn}_3\text{Ga}_{(1-x)}\text{Sn}_x\text{C}$.

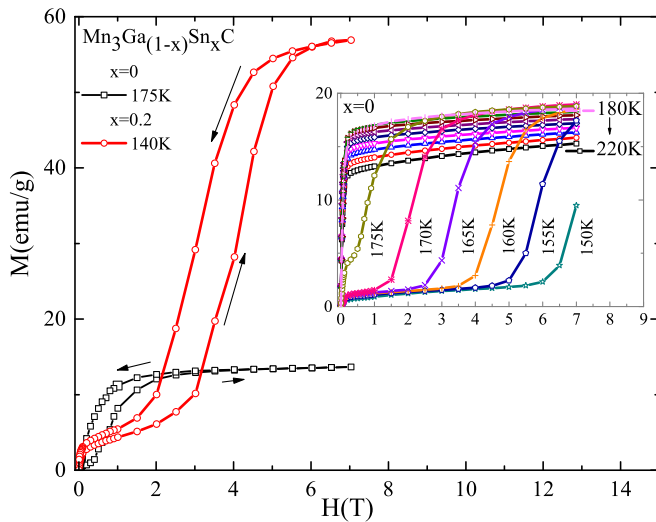


FIG. 2. Isothermal magnetization curves as a function of external magnetic field, $H \leq 7$ T for $\text{Mn}_3\text{Ga}_{(1-x)}\text{Sn}_x\text{C}$ ($x = 0$ and $x = 0.2$) compounds measured across the first order transition region.

ferromagnetic like behavior even though the compound is in AFM state ($T_N = 179$ K). The reason for such a behavior is clear from the magnetization curves present in the inset of Fig. 2. Mn_3GaC undergoes a field induced metamagnetic transition from antiferromagnetic to ferromagnetic state. The critical field value of this transition of course increases with lowering of temperature. It may be pointed out that neutron diffraction studies have shown that not only the magnetic order but also the unit cell volume returns to its pre-transition value.²⁵ This is a clear indication of coupling between magnetic and structural degrees of freedom.

For Sn doped compounds ($x \leq 0.55$), though the metamagnetic transition still occurs, the magnetic field required to induce this transition increases with Sn concentration. For example, in $x = 0.2$, the transition occurs at $H \sim 3$ T at 140 K ($T/T_N \sim 0.95$) while in $x = 0$, only 1 T magnetic field is required to induce the transition at the same relative temperature ($T = 170$ K). Furthermore, this value of magnetic field

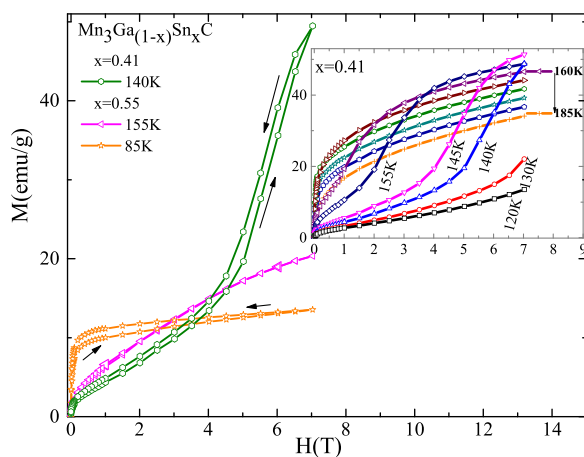


FIG. 3. Magnetization curves $M(H)$, measured across the first order transition of $\text{Mn}_3\text{Ga}_{(1-x)}\text{Sn}_x\text{C}$ with $x = 0.41$ and 0.55 as a function of external magnetic field ($H \leq 7$ T).

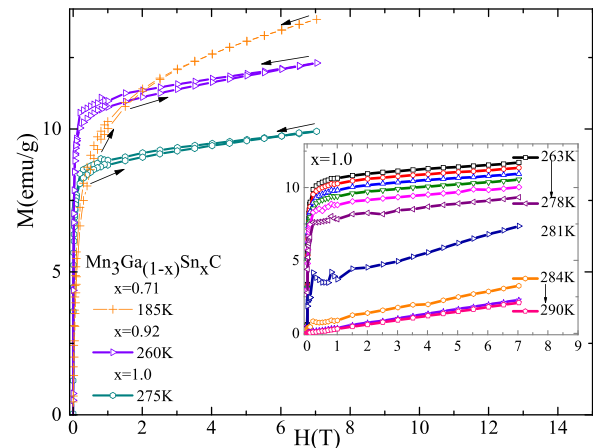


FIG. 4. $M(H)$ curves as a function of external magnetic fields ($0 \leq H \leq 7$ T) for Sn rich $\text{Mn}_3\text{Ga}_{(1-x)}\text{Sn}_x\text{C}$ compounds ($x \geq 0.71$) measured across the first order transition region.

increases to ~ 5 T in $x = 0.41$ and perhaps to more than 7 T in $x = 0.55$. For higher Sn concentration, no metamagnetic transition is seen and the magnetic order is dominated by ferromagnetic interactions. In fact, even in case of $x = 0.55$, wherein there are two first order magnetic transitions at 155 K and 85 K and which have been, respectively, attributed to Ga rich and Sn rich regions,²⁴ the transition at 85 K does not exhibit any signatures of a metamagnetic transition. At higher concentrations of Sn, FM interactions appear to strengthen and the transition temperature increases to ~ 280 K in Mn_3SnC . Such a behavior indicates that Sn doping not only strengthens the ferromagnetic interactions but at the same time weakens the AFM state. Local interactions usually play a major role in metamagnetic transitions occurring in the vicinity of a first order transition.²⁸ Therefore, it is quite intriguing to understand how Sn doping, beyond a critical concentration, changes the magnetic character of the compounds and increases the transformation temperature while completely destroying the AFM state.

We seek answers to the above through a study of magnetic entropy behaviour in $\text{Mn}_3\text{Ga}_{(1-x)}\text{Sn}_x\text{C}$. Figures 5 and 6 present a graphical representation of temperature dependence of entropy change associated with first order phase transition for $\text{Mn}_3\text{Ga}_{(1-x)}\text{Sn}_x\text{C}$ ($0 \leq x \leq 1$) compounds. ΔS_M values were calculated from magnetization isotherms near the ordering temperature using Eq. (2). As expected, the rapid change in magnetization seen at the first order transition in these materials is accompanied by maximum entropy change indicated by prominent peak like structures around the transition regions marked in Figure 1. Though the transition is clearly of first order for all compounds belonging to the series, the nature of the MCE has a strong dependence on the Sn content.

The entropy change in Ga rich compounds accompanying the first order FM-AFM transition is depicted by inverse MCE peaks in Figures 5(a) and 5(b). In Mn_3GaC ($x = 0$), as the magnetic field increases, a second peak (indicated by an arrow in Figure 5(a)) develops (for $H \geq 5$ T). Such a two peak structure has been reported in compounds with a coupled first order magnetic transition and a metamagnetic

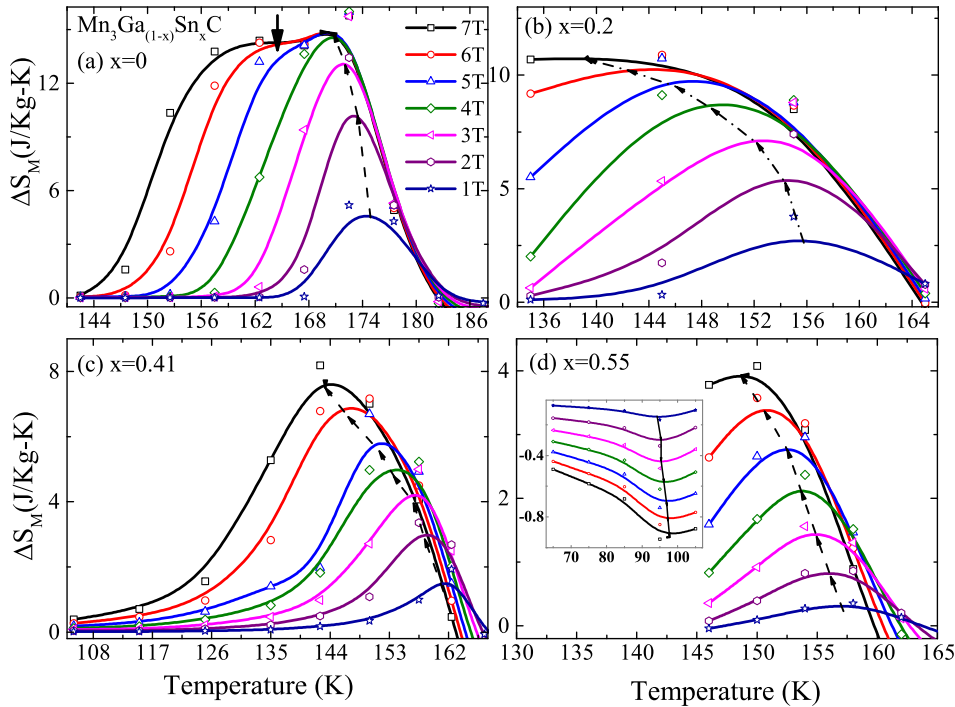


FIG. 5. Entropy change in the vicinity of the magnetostructural transition as determined from magnetization measurements for $\text{Mn}_3\text{Ga}_{(1-x)}\text{Sn}_x\text{C}$, $0 \leq x \leq 0.55$.

transition.²⁹ The observed profile in Figure 5(a) could also indicate a simple broadening of the peak for $H \geq 5$ T indicating that the whole transition is induced for this range of magnetic fields. However, a clear shift in the position of the peak towards lower temperatures with increasing magnetic field can be seen in the figure. The calculated maximum values of ΔS_M at the AFM ordering temperature and the associated adiabatic temperature difference of about $\Delta T \sim 4$ K are in fair

agreement with reported values.²² A similar nature of ΔS_M versus temperature profile can be seen in sample with 20% Sn doping. Here too, the applied field shifts the first order transition towards lower temperatures but the ΔS_M value, in comparison to undoped compound, is lower at 7.4 J/kg K ($H = 2$ T) and attains a maximum value of 10.8 J/kg K in an applied field of 7 T. Increasing the magnetic field beyond 5 T does not seem to affect the maximum MCE value, but gives rise to a table like temperature dependence of the entropy due to a coupling between the first order FM–AFM transition and the field induced AFM–FM transition.³⁰

Entropy changes as a function of temperature in various applied fields shown in Figures 5(c), 5(d), and 6(a) for three intermediate concentrations of Sn depict a strong dependence of the magnitude of ΔS_M on the nature of magnetic ordering in a material. In the case of $x = 0.41$ also the maximum of ΔS_M , $(\Delta S_M)_{max}$ shifts to lower temperatures with increasing magnetic fields. Furthermore, the increasing width of the peak also hints towards a coupling seen in Ga rich compounds. A similar behavior is also noticed for the 155 K transition in $x = 0.55$ (Figure 5(d)). However, the first order transition at 85 K in $x = 0.55$ neither exhibits broadening nor a shift in the $(\Delta S_M)_{max}$. This transition at 85 K is ascribed to the ordering of Sn rich regions, while the transition at 155 K is related to transformation of Ga rich regions.²⁴ The fact that $(\Delta S_M)_{max}$ at 155 K shows a variation in its position as a function of magnetic field and the entropy peak at 85 K does not indicate the changing nature of magnetostructural coupling due to Sn doping. This is further confirmed from the behavior of ΔS_M versus temperature curves calculated for different magnetic fields in $x = 0.71$, 0.92, and 1.0, which are presented in Figures 6(a)–6(c). In all these cases, not only the ΔS_M is negative indicating conventional magnetocaloric effect but also there is very little variation in the position of $(\Delta S_M)_{max}$ with increasing magnetic field.

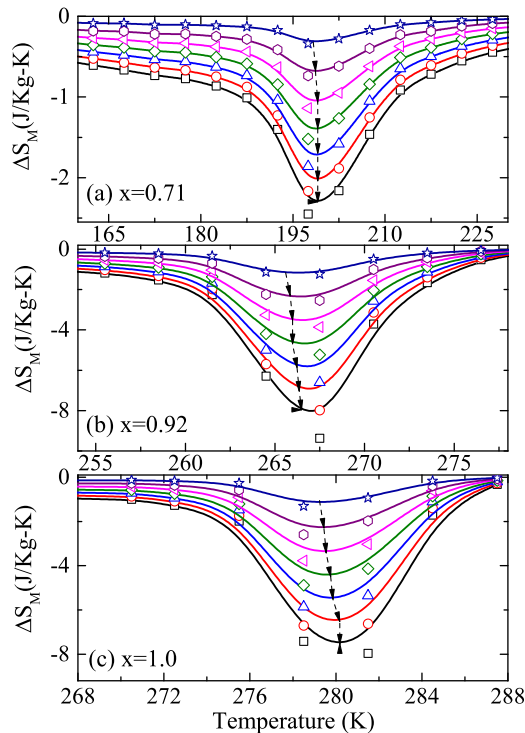


FIG. 6. Entropy change in the vicinity of the magnetostructural transition as determined from magnetization measurements for Sn rich $\text{Mn}_3\text{Ga}_{(1-x)}\text{Sn}_x\text{C}$.

IV. DISCUSSION

Magnetization measurements reveal that doping of Sn in Mn_3GaC results in evolution of FM interactions in the transformed AFM phase of Ga rich compounds along with lowering of the first order transformation temperature. The $x=0.55$ compound undergoes two first order transformations, respectively, at 155 K and 85 K, which are ascribed to Ga rich regions and Sn rich regions. With further increase in Sn concentration, the first order transition temperature rises steeply and the compounds transform from a PM to FIM state. Another notable feature is the disappearance of the field induced transition with Sn doping. Field induced AFM to FM transition is present in all Ga rich compounds ($x \leq 0.41$) but the critical field required to induce this transition increases with Sn concentration.

The metamagnetic transition in Mn_3GaC occurs from a high volume AFM state to low volume FM state.¹⁸ The replacement of Ga by larger Sn results in a natural volume expansion which not only lowers the transformation temperature but also pushes the metamagnetic transition to higher magnetic fields. These two magnetostructural transitions in Mn_3GaC are magneto-volume transitions, wherein the magnetic field plays a role akin to that of hydrostatic pressure. This is clear from the fact that in all Ga rich $\text{Mn}_3\text{Ga}_{(1-x)}\text{Sn}_x\text{C}$ ($x \leq 0.41$) compounds, the first order low volume FM to high volume AFM transition shifts to a lower temperature in presence of magnetic field. The increase in the critical field required to induce AFM-FM metamagnetic transition with increasing Sn content could, therefore, be related to the increase in unit cell volume with Sn doping. The larger the volume of the unit cells, higher the magnetic field (more pressure) required to convert them from the high volume AFM to low volume FM state.

In $x=0.55$, two first order transitions at 155 K and 85 K corresponding, respectively, to Ga rich regions and Sn rich regions are observed. The transition at 155 K shows a similar magnetic field dependence as other Ga rich compounds even though it occurs at a slightly higher temperature compared to that in $x=0.41$. While the transition at 85 K exhibits negligible field dependence, thereby supporting the argument of existence of two magnetic phases.²⁴ This behaviour can be clearly seen from the variation in temperature of peak of (ΔS_M) (T_p) as a function of magnetic field. In Figure 7, the plot of $\Delta T = T_p(H) - T_p(0.1T)$ as a function of magnetic field shows a large variation for Ga rich compounds. In the case of $x=0.55$, the transition at 155 K exhibits variation in its position with increasing magnetic field, while the transition at 85 K has a behaviour similar to that exhibited by Sn rich compounds.

Up to about $x < 0.5$, the role of Sn could be that of increasing the lattice volume. For higher Sn concentrations, its role appears to change. In spite of a steady increase in the lattice constant from Mn_3GaC to Mn_3SnC , the first order transformation temperature increases with increasing Sn concentration for $x \geq 0.5$. This is exactly opposite to the behavior of Ga rich $\text{Mn}_3\text{Ga}_{(1-x)}\text{Sn}_x\text{C}$, wherein the substitution of Sn causes the transformation temperature to decrease due to cell volume expansion. Alternately, starting with

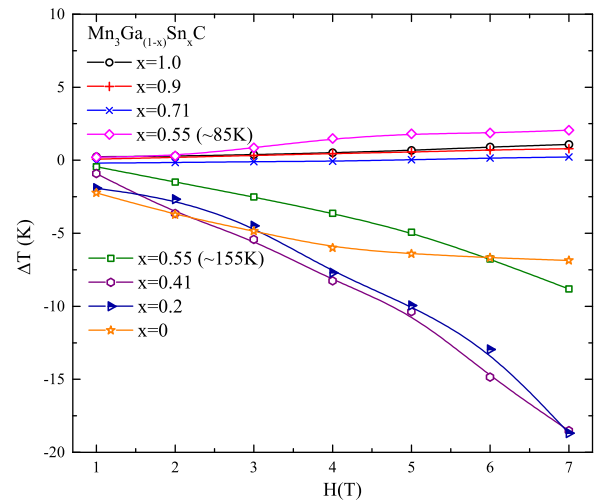


FIG. 7. Variation of ΔT as a function of applied magnetic field for $\text{Mn}_3\text{Ga}_{(1-x)}\text{Sn}_x\text{C}$ compounds.

Mn_3SnC , the decrease in first order transformation temperature due to Ga substitution can be ascribed to a decrease in unit cell volume. In itinerant electron magnetic systems, a decrease in cell volume increases the band width, which suppresses magnetic moment.^{31,32} Therefore, as the Sn content is diluted with smaller Ga, the magnetic transformation temperature decreases. Again, this explanation is valid only up to 50% Ga doping. For higher Ga concentrations, there is not only an abrupt increase in transformation temperature from 85 K to ~ 150 K, the nature of transformation also changes from PM-FIM type to FM-AFM type. This behavior points to the changing role of the A site ion in the magnetostructural transformation in antiperovskites. Such a crucial role of A site ions has also been highlighted in another family of Mn antiperovskites containing nitrogen.²⁸

Though both Mn_3GaC and Mn_3SnC are isostructural compounds undergoing a volume discontinuous first order transformation, there are many dissimilarities between them. Apart from the difference in nature of magnetic transition associated with the structural transition in the two compounds, the magnetic propagation vector as indicated by neutron diffraction studies is also different.¹⁸ In Mn_3GaC , the AFM propagation vector is along the $[\frac{1}{2}, \frac{1}{2}, \frac{1}{2}]$ direction giving rise to a collinear AFM order along the $[111]$ direction.³³ While in Mn_3SnC , the AFM order propagation vector, $\vec{k} = [\frac{1}{2}, \frac{1}{2}, 0]$, resulting in an anisotropic structure of the type $(a\sqrt{2}, a\sqrt{2}, a)$ with a square arrangement of the spins at two of the Mn sites giving rise to an AFM configuration with a small ferromagnetic component and a parallel FM component at the third site responsible for the FM like behavior.³⁴

Recent EXAFS studies have shown that the CMn_6 octahedra in Mn_3SnC is locally distorted even in the paramagnetic phase and in spite of a cubic crystal structure.³⁵ The distortion of CMn_6 octahedra gives rise to shorter and longer Mn-Mn bond distances, which critically affect the competition between nearest Mn-Mn antiferromagnetic interactions and next nearest Mn-Mn ferromagnetic interactions²⁸ and has been considered to be the reason for the change in the direction of magnetic propagation vector in Mn_3SnC with

respect to that in Mn_3GaC . Such a distortion can also be used to explain the observed behavior of magnetocaloric effect and change in the first order magnetic transformation temperature. Mn_3GaC consists of regular CMn_6 octahedra. Addition of Sn in place of Ga in Mn_3GaC results in anisotropic tensile strain in some of the CMn_6 octahedra and, therefore, makes it that much harder for the applied magnetic field to induce a magneto-volume transformation, which converts the AFM ground state to FM one. With increase in Sn concentration, therefore, the metamagnetic transition shifts to higher values of applied magnetic field. In $x = 0.55$, the two types of octahedra, unstrained (Ga rich regions) and strained (Sn rich regions), could be nearly equal in number and, hence, two first order transformations are seen. With further increase in Sn content, the number of strained octahedra exceeds the number of unstrained ones and the temperature of first order transformation increases. Therefore, the local strain introduced by the A site cation seems to play an important role in magneto-volume transformation in $\text{Mn}_3\text{Ga}_{(1-x)}\text{Sn}_x\text{C}$ antiperovskite compounds.

V. CONCLUSIONS

In summary, the paper reports a study on the nature of magnetocaloric effect in $\text{Mn}_3\text{Ga}_{(1-x)}\text{Sn}_x\text{C}$ antiperovskite compounds. It is seen that compounds rich in Ga content exhibit a strong magnetic field dependence of the FM-AFM transformation as well as a field induced magneto-volume transformation from AFM to FM state. Such a field dependence of first order transition as well as metamagnetic transition is absent in Sn rich compounds. This has been shown to be due to a local strain introduced by substitution of larger Sn in place of Ga. Presence of such a local strain introduces FM interactions through a change in magnetic propagation vector and, hence, the first order transformation temperature decreases. A suppression of metamagnetic transition is also seen with increasing Sn concentration. With increase in Sn concentration beyond $x = 0.5$, the higher number of strained CMn_6 octahedra causes the first order transformation temperature to increase with increase in Sn content.

ACKNOWLEDGMENTS

Authors thank Board of Research in Nuclear Sciences (BRNS) for the financial support under the Project 2011/37P/06. M/s. Devendra D. Buddhikot, and Ganesh Jangam are acknowledged for the experimental assistance.

¹V. K. Pecharsky and K. A. Gschneidner, Jr., *J. Magn. Magn. Mater.* **200**, 44 (1999).

²D. Bourgault, J. Tillier, P. Courtois, X. Chaud, N. Caillault, and L. Carbone, *Phys. Procedia* **10**, 120 (2010).

- ³J. S. Amaral and V. S. Amaral, *J. Magn. Magn. Mater.* **322**, 1552 (2010).
- ⁴V. K. Pecharsky and K. A. Gschneidner, Jr., *Phys. Rev. Lett.* **78**, 4494 (1997).
- ⁵E. Brück, O. Tegus, D. T. C. Thanh, N. T. Trung, and K. H. J. Buschow, *Int. J. Refrig.* **31**, 763 (2008).
- ⁶V. K. Pecharsky, K. A. Gschneidner, Jr., Y. Mudryk, and D. Paudyal, *J. Magn. Magn. Mater.* **321**, 3541 (2009).
- ⁷X. X. Zhang, J. Tejada, Y. Xin, G. F. Sun, K. W. Wong, and X. Bohigas, *Appl. Phys. Lett.* **69**, 3596–3598 (1996).
- ⁸M. Annaorazov, K. Asatryan, G. Myalikgulyev, S. Nikitin, A. Tishin, and A. Tyurin, *Cryogenics* **32**, 867 (1992).
- ⁹O. Tegus, E. Brück, L. Zhang, Dagula, K. H. J. Buschow, and F. R. de Boer, *Phys. B* **319**, 174 (2002).
- ¹⁰F.-X. Hu, B.-G. Shen, and J.-R. Sun, *Appl. Phys. Lett.* **76**, 3460–3462 (2000).
- ¹¹F.-X. Hu, B.-G. Shen, J.-R. Sun, and G.-H. Wu, *Phys. Rev. B* **64**, 132412 (2001).
- ¹²A. Planes, L. Mañosa, and M. Acet, *J. Phys.: Condens. Matter* **21**, 233201 (2009).
- ¹³F.-X. Hu, B.-G. Shen, J.-R. Sun, and Z.-H. Cheng, *Phys. Rev. B* **64**, 012409 (2001).
- ¹⁴F.-X. Hu, B.-G. Shen, J.-R. Sun, Z.-H. Cheng, G.-H. Rao, and X.-H. Zhang, *Appl. Phys. Lett.* **78**, 3675–3677 (2001).
- ¹⁵O. Tegus, E. Brück, K. H. J. Buschow, and F. R. de Boer, *Nature* **415**, 150 (2002).
- ¹⁶F.-X. Hu, B.-G. Shen, J.-R. Sun, G.-J. Wang, and Z.-H. Cheng, *Appl. Phys. Lett.* **80**, 826–828 (2002).
- ¹⁷J. Bouchaud, R. Fruchart, R. Pauthenet, M. Guillot, H. Bartholin, and F. Chais, *J. Appl. Phys.* **37**, 971–972 (1966).
- ¹⁸D. Fruchart and E. F. Bertaut, *J. Phys. Soc. Jpn.* **44**, 781 (1978).
- ¹⁹J. García, J. Bartolomé, D. González, R. Navarro, and D. Fruchart, *J. Chem. Thermodyn.* **15**, 1059 (1983).
- ²⁰T. Tohei, H. Wada, and T. Kanomata, *J. Appl. Phys.* **94**, 1800–1802 (2003).
- ²¹B. S. Wang, P. Tong, Y. P. Sun, X. Luo, X. B. Zhu, G. Li, X. D. Zhu, S. B. Zhang, Z. R. Yang, W. H. Song, and J. M. Dai, *EPL* **85**, 47004 (2009).
- ²²E. Dias, K. Priolkar, and A. Nigam, *J. Magn. Magn. Mater.* **363**, 140 (2014).
- ²³Ö. Çakir and M. Acet, *J. Magn. Magn. Mater.* **344**, 207 (2013).
- ²⁴E. T. Dias, K. R. Priolkar, and A. K. Nigam, *Mater. Res. Express* **1**, 026106 (2014).
- ²⁵Ö. Çakir, M. Acet, M. Farle, and A. Senyshyn, *J. Appl. Phys.* **115**, 043913 (2014).
- ²⁶K. A. Gschneidner and V. K. Pecharsky, *Annu. Rev. Mater. Sci.* **30**, 387 (2000).
- ²⁷A. Morrish, *The Physical Principles of Magnetism*, Wiley Series on the Science and Technology of Materials (Wiley, 1965).
- ²⁸K. Takenaka, M. Ichigo, T. Hamada, A. Ozawa, T. Shibayama, T. Inagaki, and K. Asano, *Sci. Technol. Adv. Mater.* **15**, 015009 (2014).
- ²⁹E. K. Liu, Z. Y. Wei, Y. Li, G. D. Liu, H. Z. Luo, W. H. Wang, H. W. Zhang, and G. H. Wu, *Appl. Phys. Lett.* **105**, 062401 (2014).
- ³⁰M.-H. Yu, L. H. Lewis, and A. R. Moodenbaugh, *J. Appl. Phys.* **93**, 10128–10130 (2003).
- ³¹E. F. Wasserman, in *Handbook of Ferromagnetic Materials*, edited by K. Buschow and E. Wohlfarth (Elsevier, 1990), Vol. 5, pp. 237–322.
- ³²Y. Takahashi and H. Nakano, *J. Phys.: Condens. Matter* **18**, 521 (2006).
- ³³D. Fruchart, E. Bertaut, F. Sayetat, M. N. Eddine, R. Fruchart, and J. Sneath, *Solid State Commun.* **8**, 91 (1970).
- ³⁴P. l'Heritier, J. P. Senateur, R. Fruchart, D. Fruchart, and E. F. Bertaut, *Mater. Res. Bull.* **12**, 533 (1977).
- ³⁵E. T. Dias, K. R. Priolkar, A. Das, G. Aquilanti, Ö. Çakir, M. Acet, and A. K. Nigam, preprint [arXiv:1502.04448](https://arxiv.org/abs/1502.04448) (2015).